Journal of Southeast University (English Edition) Vol. 21, No. 1, pp. 78 - 81 Mar. 2005 ISSN 1003—7985

# Behavior of soil lateral deformation under embankments

Yu Chuang Liu Songyu

(College of Transportation, Southeast University, Nanjing 210096, China)

**Abstract:** Based on analysis of additional horizontal stress in the soil under embankment load, the behavior of the lateral deformation of the soil along the depth is studied. The result shows that the distribution of lateral deformation along the depth is arch-shaped, which corresponds nicely with the observed data. According to this, a new prediction model is established to forecast the lateral deformation. The shapes of the model curve with three parameters in the model $a$, $b$ and $c$ are presented. The three parameters can easily be determined by three measured data $(s_0, 0)$, $(s_1, h_0)$ and $(s_2, 2h_0)$. This model is applied to study two cases. The comparisons illustrate that the displacement predicted by the model corresponds nicely with the measured data.

**Key words:** lateral deformation; embankment; prediction; additional stress

In the highway construction on soft ground, the stability and settlement of the subsoil should be considered; the latter is more complicated. The lateral deformation of soft soil always exists under embankment load, which not only affects the vertical settlement, but also affects the behavior of adjacent structures[1-3]. Larger lateral deformation even influences the stability of the ground. The lateral deformation can be considered a good indicator of the stability of embankment foundations, and many scholars[4-6] have researched this aspect. Based on the characteristics of lateral deformation along the depth, a new prediction model is established to forecast the lateral deformation. The model is applied to two cases and the model can predict the lateral deformation subject to embankment load reliably.

## 1 Characteristics of Additional Horizontal Stress in Soil under Embankments

The additional stress, which is the main cause of the deformation in the soil under embankment load (see Fig. 1), can be solved by the following equations[7].

$$\sigma_x = \frac{p}{\pi}\left[\beta + \frac{x\alpha}{a} + \frac{z}{r_2^2}(x-b) + \frac{2z}{a}\ln\frac{r_1}{r_0}\right] \quad (1)$$

$$\sigma_z = \frac{p}{\pi}\left[\beta + \frac{x\alpha}{a} - \frac{z}{r_2^2}(x-b)\right] \quad (2)$$

$$\tau_{xz} = -\frac{p}{\pi}\left(\frac{z\alpha}{a} - \frac{z^2}{r_2^2}\right) \quad (3)$$

where the above parameters are shown in Fig. 1.

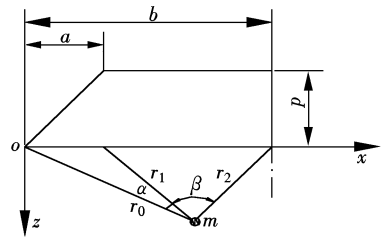


**Fig. 1** Sketch of uniform embankment load

For the typical embankment load, as indicated in Fig. 2, the point $m(0, z)$ where the additional horizontal stress produced by the shadow part load, can be obtained by Eq. (1). For symmetry, the additional horizontal stress produced by the other part load can be obtained through the point $m'(2b, z)$ by the shadow part load. Then the additional horizontal stress at the point $m$ can be obtained by

$$\sigma_{mx} = \frac{p}{\pi}\left(\arctan\frac{b}{z} - \arctan\frac{a}{z} - \frac{z}{z^2+b^2}b + \frac{2z}{a}\ln\frac{\sqrt{z^2+a^2}}{z}\right) + \frac{p}{\pi}\left[\arctan\frac{2b-a}{z} + \frac{2b}{a}\left(\arctan\frac{2b}{z} - \arctan\frac{2b-a}{z}\right) + \frac{1}{z}b + \frac{2z}{a}\ln\frac{\sqrt{z^2+(2b-a)^2}}{\sqrt{z^2+4b^2}}\right] \quad (4)$$

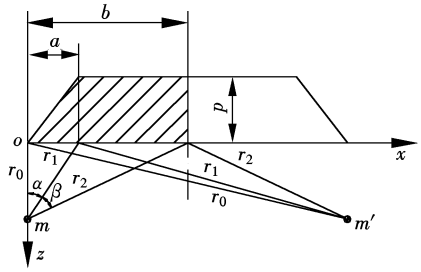


**Fig. 2** Sketch of embankment load in highway

**Received** 2004-08-27.

**Foundation item:** The Ph. D. Programs Foundation of Ministry of Education of China (No. 2001028618).

**Biographies:** Yu Chuang (1977—), male, graduate; Liu Songyu (corresponding author), male, doctor, professor, liusy@seu.edu.cn.

Thus the additional horizontal stress along the depth at the toe under embankment load can be expressed by Eq. (4).

Eq. (4) is too complicated. It can be intuitively shown in Fig. 3, as $h = 5$ m ($h$ is the embankment height), $a = 7.5$ m, $b = 22.5$ m, $p = 100$ kPa. And the curve is arch-shaped. $\varepsilon = \sigma/E$ (elastical module), when the value of $E$ remains constant along the depth, the distribution of lateral deformation is the same as the additional horizontal stress. For the homogeneous subsoil, the distribution of lateral deformation is also arch-shaped.

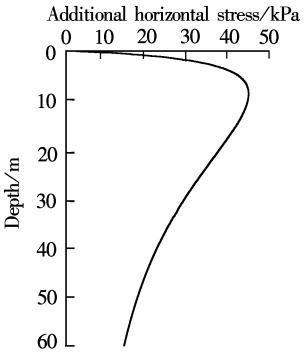


**Fig. 3** Distribution with the depth of the additional horizontal stress under embankments

## 2 Behavior and Prediction of Soil Lateral Deformation under Embankments

### 2.1 Analysis on the observed data

Tavenas, et al. [8] has summarized the lateral deformation developing in clay foundations under 21 different embankments, and the relationship between the lateral deformation and vertical settlement is analyzed. The typical curve of the lateral deformation with the depth is shown in Fig. 4. It is clear that the maximum lateral deformation occurs not on the surface but in a place below the surface.

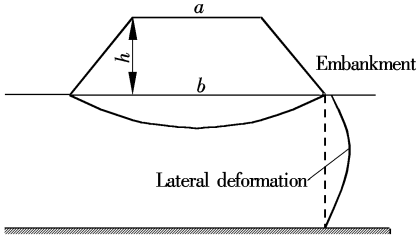


**Fig. 4** Typical deformation pattern in embankment foundation

After long-term observations, Tavenas, et al. [9] presented the ratio $y/y_m$ with the depth, see Fig. 5. Plenty of measured data show that the distribution of lateral deformation with the depth is arch-shaped and the maximum deformation exists at some distance under the ground.

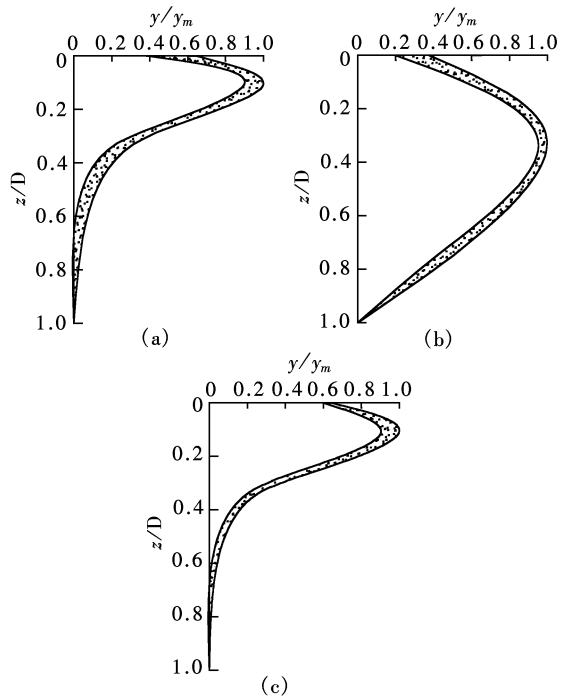


**Fig. 5** Lateral deformation distribution with the depth under embankments. (a) Saint-Alban-B; (b) Cubzac-Ponts-B; (c) Ska-Edeby

### 2.2 Establishment of the prediction model

Based on the additional horizontal stress distribution with the depth in the soil under the embankment load and the measured data, it can be obviously concluded that the curve of lateral deformation with the depth is arch-shaped. The following function is presented to predict the lateral deformation.

$$s = (a + bz)\,e^{-cz} \tag{5}$$

where $a$, $b$ and $c$ are the parameters in the model, and $z$ is the depth.

This function matches the characteristic of the shape of the lateral deformation, and owes good adaptability. Figs. 6(a), (b) and (c) show the curves of the model varying with the three parameters, respectively.

1) When $z = 0$, $s = a \neq 0$, that is the value of the lateral deformation at the ground surface, which is accorded to the above analysis.

2) The differentiation of the model equation $s$ with respect to the depth $z$ is shown by Eq. (6). When $z \leqslant (b - ac)/bc$, $s' \geqslant 0$ demonstrating that the lateral deformation increases with the depth. When $z > (b - ac)/bc$, $s' < 0$ representing that the lateral deformation decreases with the increase of the depth.

$$\frac{\partial s}{\partial z} = (b - ac - bcz)\,e^{-cz} \tag{6}$$

3) The second derivative $s$ to $z$ is expressed by Eq. (7). When $z \leqslant (2b - ac)/bc$, $s'' \leqslant 0$, and when $z > (2b - ac)/bc$, $s'' > 0$. The second derivative chan-

ges from a negative quantity to a positive quantity, so the curve has an inflexion. It is arch-shaped.

$$\frac{\partial^2 s}{\partial z^2} = (ac^2 - 2bc + bc^2 z)\,\mathrm{e}^{-cz} \tag{7}$$

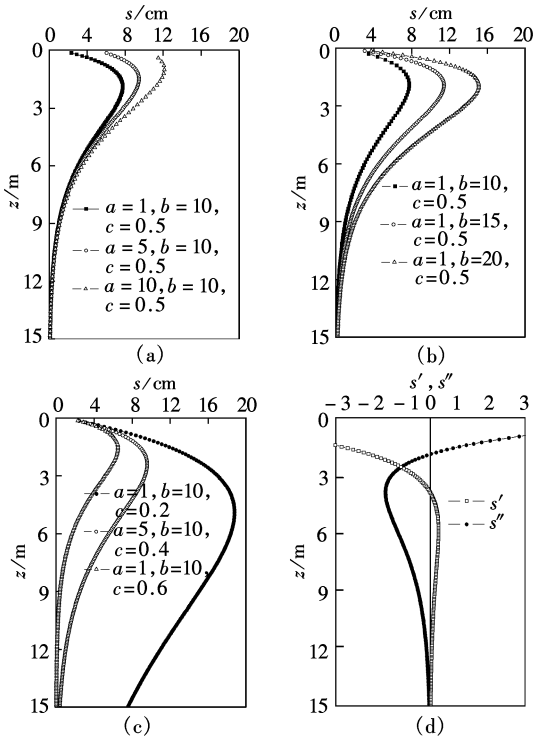


**Fig. 6** Behavior of the curves. (a) Shape with parameter $a$; (b) Shape with parameter $b$; (c) Shape with parameter $c$; (d) The first and the second derivative

Fig. 6(d) gives the curves of the first derivative and the second derivative. The first derivative changes from a positive quantity to a negative quantity, so the deformation increases at first then decreases with depth. The second derivative changes from a negative quantity to a positive quantity, so the curve has an inflexion.

### 2.3 Determination of the parameters in the prediction model

From the above analysis, it can be seen that the characteristics of the model corresponds nicely with those of the measured lateral deformation along the depth. The proper determination of the three parameters is the key to the accuracy of the model.

In Eq. (5), when $z = 0$, $a = s_{z=0}$ is the lateral deformation at the surface. The parameter $a$ can easily be determined by the lateral deformation on the surface.

Eq. (5) can be expressed as

$$s\mathrm{e}^{cz} = a + bz \tag{8}$$

Take $(s_1, h_0)$ and $(s_2, 2h_0)$ into Eq. (8), then

$$s_1\mathrm{e}^{ch_0} = a + bh_0 \tag{9}$$

$$s_2\mathrm{e}^{c2h_0} = a + 2bh_0 \tag{10}$$

Combining Eq. (9) and Eq. (10), the following equation is obtained.

$$s_2\mathrm{e}^{c2h_0} - 2s_1\mathrm{e}^{ch_0} = -a$$

where $x = \mathrm{e}^{ch_0}$, then

$$s_2x^2 - s_1x + a = 0$$

$$x = \frac{s_1 \pm \sqrt{s_1^2 - 4s_2a}}{2s_2} \qquad \text{for } x = \mathrm{e}^{ch_0}$$

so $x > 1$, $c = \ln x/h_0$, then taking $a$ and $c$ into Eq. (8), $b$ can be solved.

From the three measured data $(s_0, 0)$, $(s_1, h_0)$ and $(s_2, 2h_0)$, the three parameters in the model can be determined, then the prediction curve of the lateral deformation with the depth is obtained.

## 3 Case Analysis

### 3.1 Prediction of the lateral deformation of Hangyong highway[10]

Hangyong highway is a 145 km long major arterial road connecting Hangzhou with Ningbo, where soft clay exists along the highway. The curve of the lateral deformation with the depth of one section is shown in Fig. 7(a), which is obviously arch-shaped. The location of the maximum lateral deformation occurs at a depth of about 7 m. The predicted lateral deformation beneath the toe of the embankment is shown in Fig. 7(a). The prediction model presented in this paper well reflects the behavior of the lateral deformation along the depth.

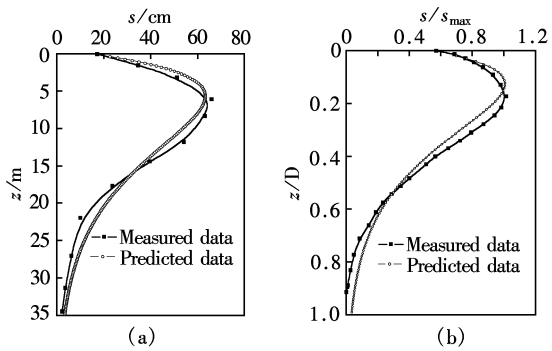


**Fig. 7** Prediction of the lateral deformation of highway. (a) Hangyong highway; (b) Nagareyama and Toichi highway

### 3.2 Prediction of the lateral deformation of Nagareyama and Toichi highway

Suzuki[11] has fully depicted the lateral deformation in Nagareyama and Toichi highway. Fig. 7(b) is one typical normalization curve of the lateral deformation with the depth. It is clear that the curve of the lateral deformation along the depth is arch-shaped. And the predicted model corresponds nicely with the observed lateral deformation along the depth.

## 4 Conclusion

The prediction of lateral deformation under the toe of an embankment during construction is possible with the model presented in this paper. On the basis of the additional horizontal stress in the soil under embankment load and plenty of measured data, a new prediction model is established. The three parameters in the model, $a$, $b$ and $c$, can easily be determined. The model is applied to study two cases. The comparisons illustrate that the lateral deformation predicted by the model corresponds nicely with the measured data. In general, the prediction of lateral deformation by the model is reliable in comparison with the observed data.

## References


[1] Yan Ke, Zhu Zhangqi, Wang Lianmin. Analysis of lateral displacement in soft soil deposits under fill construction of Haicang highway [J]. *Rock and Soil Mechanics*, 2003, **24** (suppl): 465 − 468. (in Chinese)

[2] Ma Shidong. Stability and settlement of embankment filled with stabilized light soil [J]. *Rock and Soil Mechanics*, 2003, **24**(3): 331 − 334. (in Chinese)

[3] Smadi Malek M. Lateral deformation and associated settlement resulting from embankment loading of soft clay and silt deposits [D]. Urbana, Illinois: University of Illinois, 2001.

[4] Loganathan N, Balasubramaniam A S, Bergado D T. Deformation analysis of embankments [J]. *Journal of Geotechnical Engineering*, 1993, **119**(8): 1105 − 1106.

[5] Hunter Gavan, Fell Robin. Prediction of impending failure of embankments on soft ground [J]. *Canadian Geotechnical Journal*, 2003, **40**(1): 209 − 220.

[6] Indraratna B, Balasubramaniam A S, Sivaneswaran N. Analysis of settlement and lateral deformation of soft clay foundation beneath two full-scale embankments [J]. *International Journal for Numerical and Analytical Methods in Geomechanics*, 1997, **21**(9): 599 − 618.

[7] Poulos H G, Davis E H. *Elastic solutions for soil and rock mechanics*[M]. John Wiley & Sons, Inc., 1974.

[8] Tavenas F, Mieussens C, Bourges F. Lateral displacements in clay foundations under embankments [J]. *Canadian Geotechnical Journal*, 1979, **16**(3): 532 − 550.

[9] Tavenas F, Leroueil S. Behavior of embankments on soft foundations[J]. *Canadian Geotechnical Journal*, 1980, **17** (2): 236 − 259.

[10] Cai Tileng. *Soft soil foundation improvement in Hangyong expressway* [M]. Hangzhou: Hangzhou People's Press, 1998. (in Chinese)

[11] Suzuki Otohiko. The lateral flow of soil caused by banking of soft clay ground[J]. *Soils and Foundations*, 1988, **28**(4): 1 − 11.


# 路堤下土体侧向变形性状研究


余 闯 刘松玉

(东南大学交通学院, 南京 210096)



**摘要**: 分析了路堤荷载作用下土中水平向附加应力随深度的变化特征, 得出了侧向变形沿深度"弓"形分布的变化规律, 大量实测结果也证明了这一点. 在此基础上提出了符合该变形规律的预测模型, 分析了模型曲线随其中 3 个参数 $a$, $b$ 和 $c$ 的变化规律, 并且通过 3 个实测点的侧向变形数据 $(s_0, 0)$, $(s_1, h_0)$ 和 $(s_2, 2h_0)$ 就可以简单地定出模型中这 3 个参数. 将该模型应用到 2 个工程实例当中, 预测结果和实测数据比较吻合, 取得了较好的效果.



**关键词**: 侧向变形; 路堤; 预测; 附加应力

**中图分类号**: TU433